

# Enhancement of birefringence and refractive index dispersion optimization from iodates to fluorooxiodates

Shibin Wang,<sup>a,#</sup> Jie Zhang,<sup>a,#</sup> Jianbang Chen<sup>a</sup>, Peng Han<sup>b</sup>, Na Lei<sup>b</sup> and Xuchu Huang<sup>a,\*</sup>

<sup>a</sup>College of Physics and Material Science, Changji University, Changji 831100, China.

<sup>b</sup>Xinjiang New Aluminum Industry Co., Ltd , 832000

<sup>#</sup>These authors contributed equally to this work.

\*Corresponding authors, E-mails: hxuchu@163.com

## Contents

Table S1. The main properties of  $\text{MIO}_3$  and  $\text{MIO}_2\text{F}_2$  ( $\text{M} = \text{Na}, \text{K}, \text{Rb}, \text{Cs}$ ), “Band gap-cal” shows the calculated band gap results for CASTEP, “Birefringence @1064 (nm)” shows the calculated refractive index results for CASTEP, and “Band gap-Exp/HSE06” shows the experimental band gap or the result calculated by the hybrid correlation functional HSE06.

Figure S1-S3. The structure of  $\text{MIO}_3$  ( $\text{M} = \text{K}, \text{Rb}, \text{Cs}$ ) and  $\text{MIO}_2\text{F}_2$  ( $\text{M} = \text{K}, \text{Rb}, \text{Cs}$ ).

Figure S4-S6. The TDOS and PDOS of  $\text{MIO}_3$  ( $\text{M} = \text{K}, \text{Rb}, \text{Cs}$ ) and  $\text{MIO}_2\text{F}_2$  ( $\text{M} = \text{K}, \text{Rb}, \text{Cs}$ ).

Figure S7. The angle between the lone pair electrons direction and the optical principal axis of  $\text{MIO}_3$  ( $\text{M} = \text{Na}, \text{K}, \text{Rb}, \text{Cs}$ ) and  $\text{MIO}_2\text{F}_2$  ( $\text{M} = \text{Na}, \text{K}, \text{Rb}, \text{Cs}$ ).

Figure S8-S9. The chromatic dispersion and of  $\text{MIO}_3$  ( $\text{M} = \text{Rb}, \text{Cs}$ ) and  $\text{MIO}_2\text{F}_2$  ( $\text{M} = \text{Rb}, \text{Cs}$ ).

Figure S10-S12. Structural arrangement of microscopic units of  $\text{MIO}_3$ ,  $\text{MIO}_2\text{F}_2$  ( $\text{M} = \text{K}, \text{Rb}, \text{Cs}$ ) in the direction of maximum and minimum refractive index.

Figure S13-S14. Refractive index dispersion of different NLO iodates, from  $\text{RbIO}_3$ ,  $\text{CsIO}_3$ ,  $\text{RbIO}_2\text{F}_2$  and  $\text{CsIO}_2\text{F}_2$ .

Table S1. The main properties of  $\text{MIO}_3$  and  $\text{MIO}_2\text{F}_2$  ( $\text{M} = \text{Na}, \text{K}, \text{Rb}, \text{Cs}$ ), “Band gap-cal” shows the calculated band gap results for CASTEP, “Birefringence @1064 (nm)” shows the calculated refractive index results for CASTEP, and “Band gap-Exp/HSE06” shows the experimental band gap or the result calculated by the hybrid correlation functional HSE06.

Formula	$\text{NaIO}_3^1$	$\text{NaIO}_2\text{F}_2^2$	$\text{KIO}_3^3$	$\text{KIO}_2\text{F}_2^4$	$\text{RbIO}_3^5$	$\text{RbIO}_2\text{F}_2^5$	$\text{CsIO}_3^6$	$\text{CsIO}_2\text{F}_2^6$
Structure Type	CS	CS	NCS	NCS	NCS	NCS	NCS	NCS
Space Group	<i>Pbmm</i> (62)	<i>Cmcm</i> (63)	<i>R3R</i> (146)	<i>Pca21</i> (29)	<i>R3mH</i> (160)	<i>Pca21</i> (29)	<i>R3mH</i> (160)	<i>Pca21</i> (29)
a(Å)	5.7500(3)	6.9287(10)	8.9481(8)	8.39430(4)	6.413(2)	8.567(4)	6.6051(10)	8.781(3)
b(Å)	6.3953(3)	7.2735(13)	8.9481(8)	5.97918(5)	6.413(2)	6.151(3)	6.6051(10)	6.3771(18)
c(Å)	8.1280(4)	7.3503(13)	8.9481(8)	8.44680(3)	7.854(2)	8.652(4)	8.087(3)	8.868(3)
$\alpha$ (deg)	90	90	89.950(10)	90	90	90	90	90
$\beta$ (deg)	90	90	89.950(10)	90	90	90	90	90
$\gamma$ (deg)	90	90	89.950(10)	90	120	90	120	90
V(Å <sup>3</sup> )	298.89[Å <sup>3</sup> ]	370.42[Å <sup>3</sup> ]	716.46[Å <sup>3</sup> ]	423.95[Å <sup>3</sup> ]	279.73[Å <sup>3</sup> ]	455.92[Å <sup>3</sup> ]	305.54[Å <sup>3</sup> ]	496.58[Å <sup>3</sup> ]
Z	4	4	8	4	3	4	3	4
Band gap-Cal (eV)	3.555	4.331	2.504	4.39	2.985	4.393	3.188	4.325
Band gap- HSE06 (eV)	5.128	5.806	4.303	5.899	4.394	5.908	4.574	5.912
Birefringence @1064 (nm)	0.219	0.249	0.051	0.024	0.192	0.022	0.185	0.016
Band gap-Exp (eV)	/	/	/	/	4	4.2	4.2	4.5
PM wavelength	263	217	506	526	275	535	266	595

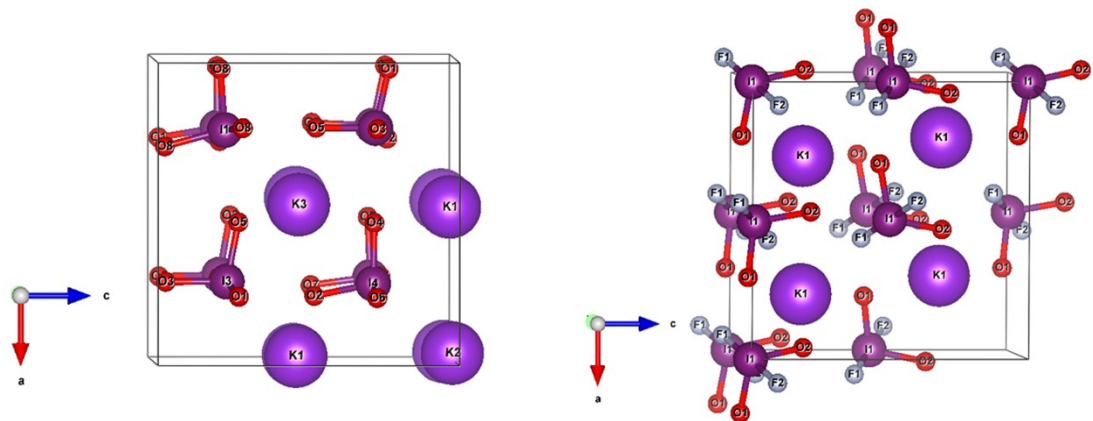


Figure S1. Structure diagram of  $\text{KIO}_3$  (left) and  $\text{KIO}_2\text{F}_2$  (right).

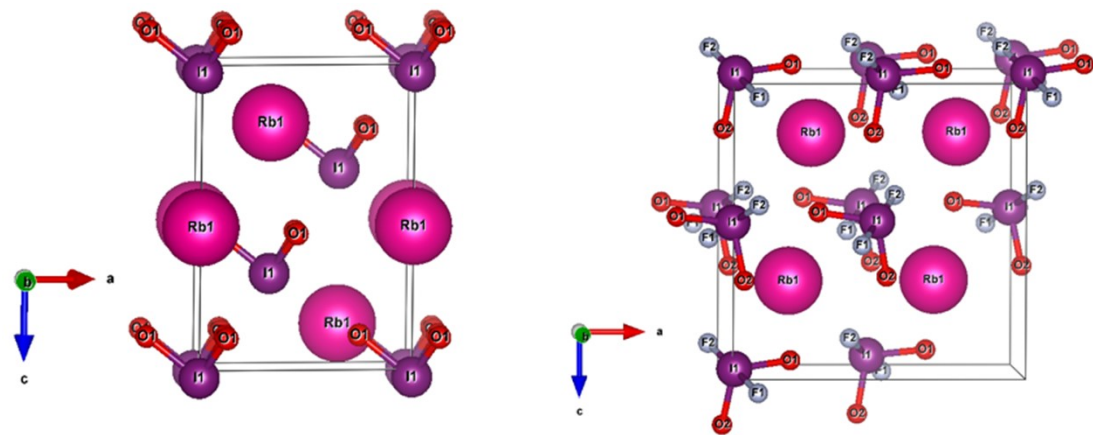


Figure S2. Structure diagram of  $\text{RbIO}_3$  (left) and  $\text{RbIO}_2\text{F}_2$  (right).

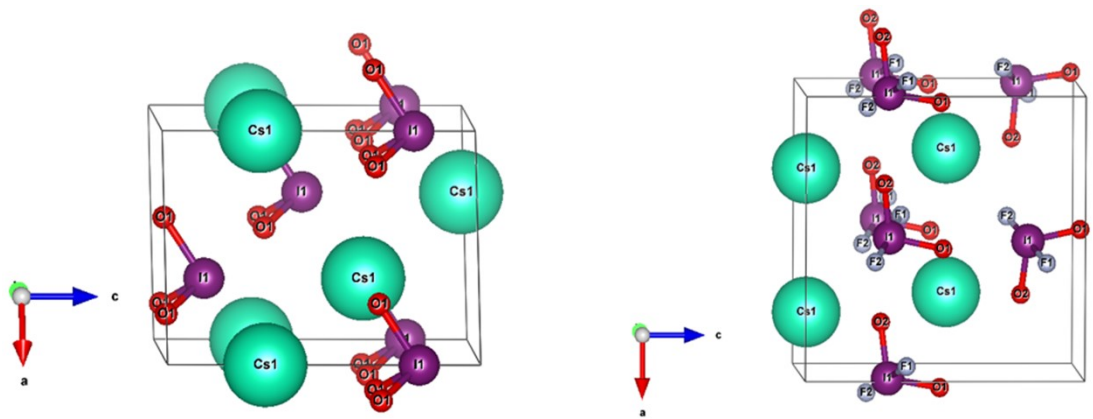


Figure S3. Structure diagram of  $\text{CsIO}_3$  (left) and  $\text{CsIO}_2\text{F}_2$  (right).

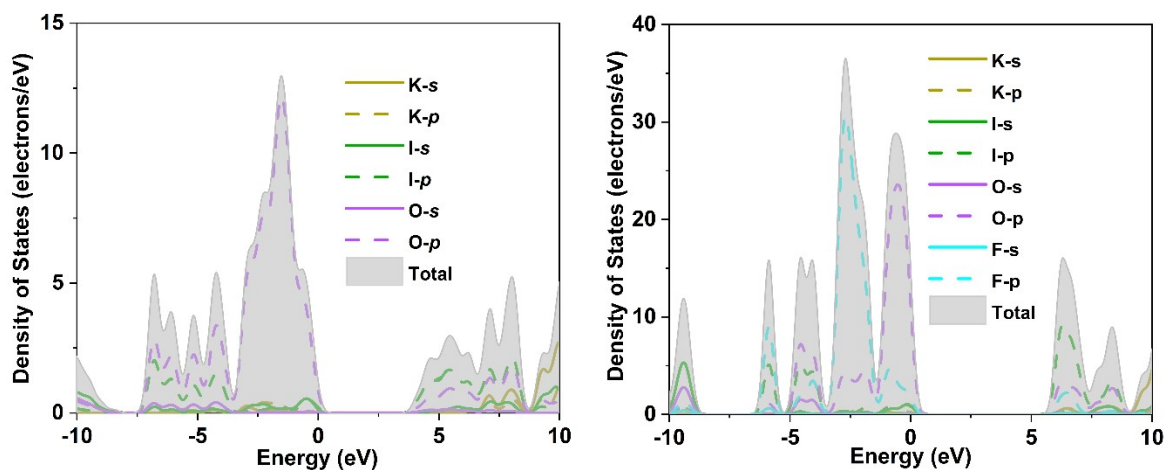


Figure S4. The PDOS of  $\text{KIO}_3$  (left) and  $\text{KIO}_2\text{F}_2$  (right).

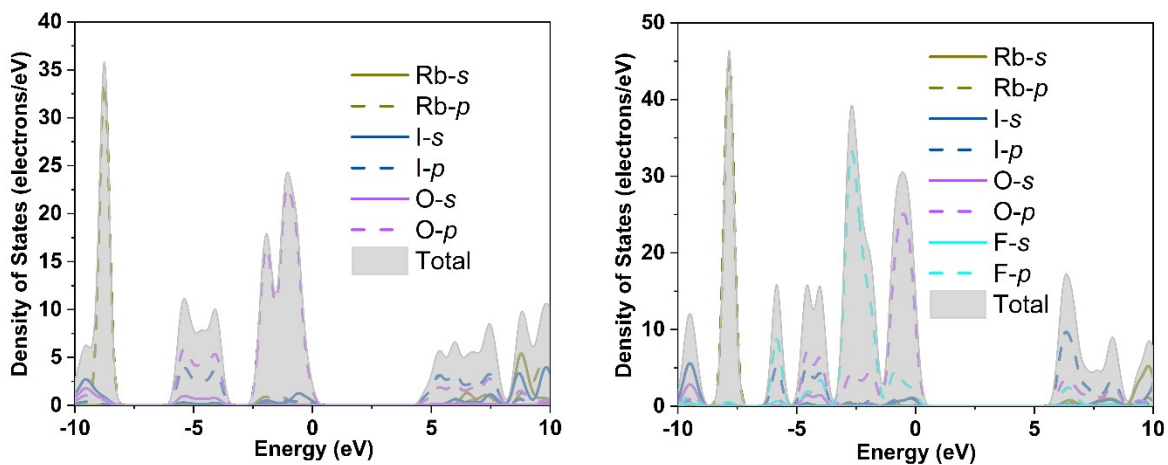


Figure S5. The PDOS of  $\text{RbIO}_3$  (left) and  $\text{RbIO}_2\text{F}_2$  (right).

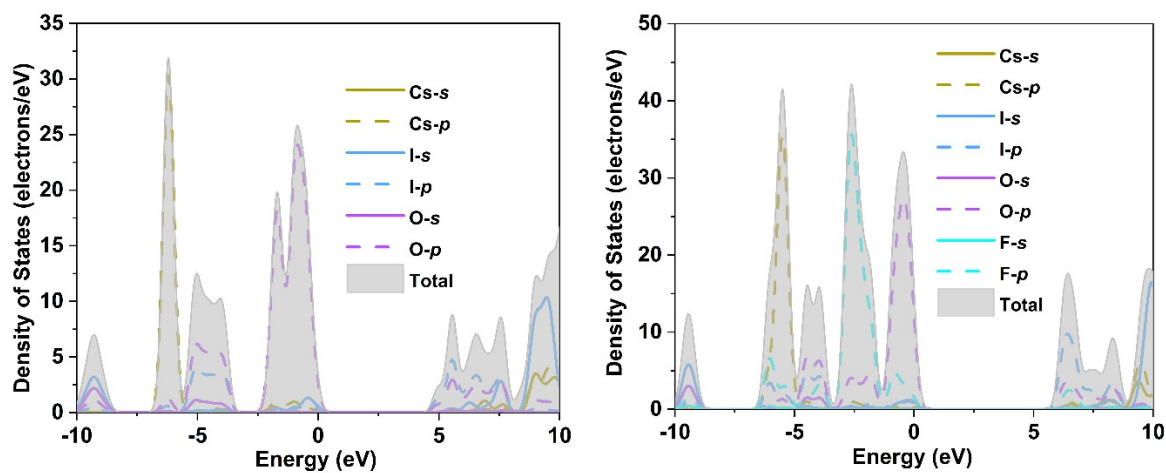


Figure S6. The PDOS of  $\text{CsIO}_3$  (left) and  $\text{CsIO}_2\text{F}_2$  (right).

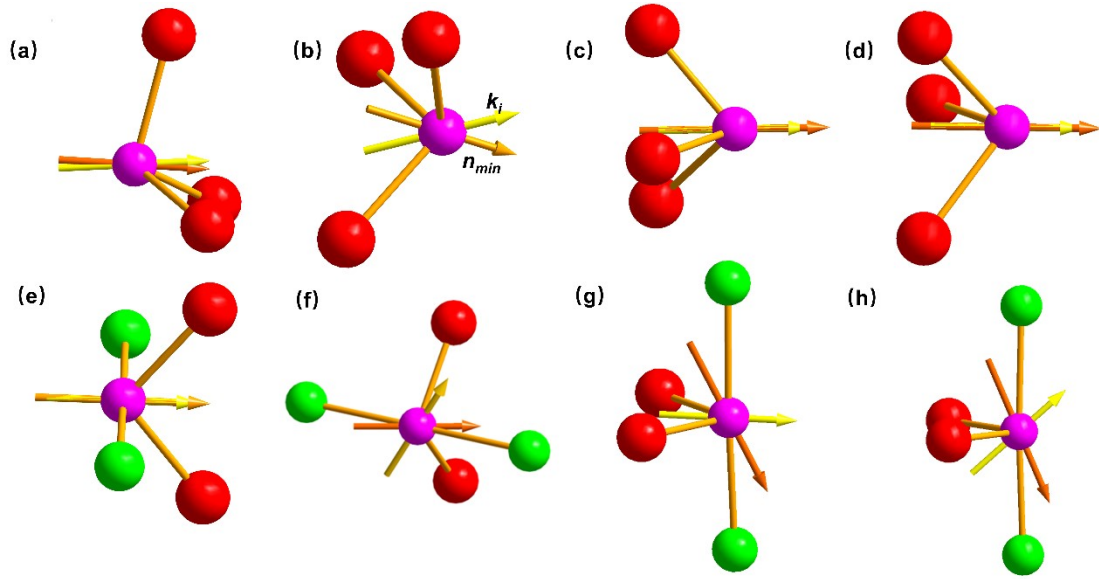


Figure S7. The angle between the lone pair electrons direction and the optical principal axis of  $\text{MIO}_3$  ( $M = \text{Na}, \text{K}, \text{Rb}, \text{Cs}$ ) and  $\text{MIO}_2\text{F}_2$  ( $M = \text{Na}, \text{K}, \text{Rb}, \text{Cs}$ ). a-h are  $\text{NaIO}_3$ ,  $\text{KIO}_3$ ,  $\text{RbIO}_3$ ,  $\text{CsIO}_3$ ,  $\text{NaIO}_2\text{F}_2$ ,  $\text{KIO}_2\text{F}_2$ ,  $\text{RbIO}_2\text{F}_2$ ,  $\text{CsIO}_2\text{F}_2$ , respectively. O (Red), I (Pink), F (Bright Green)

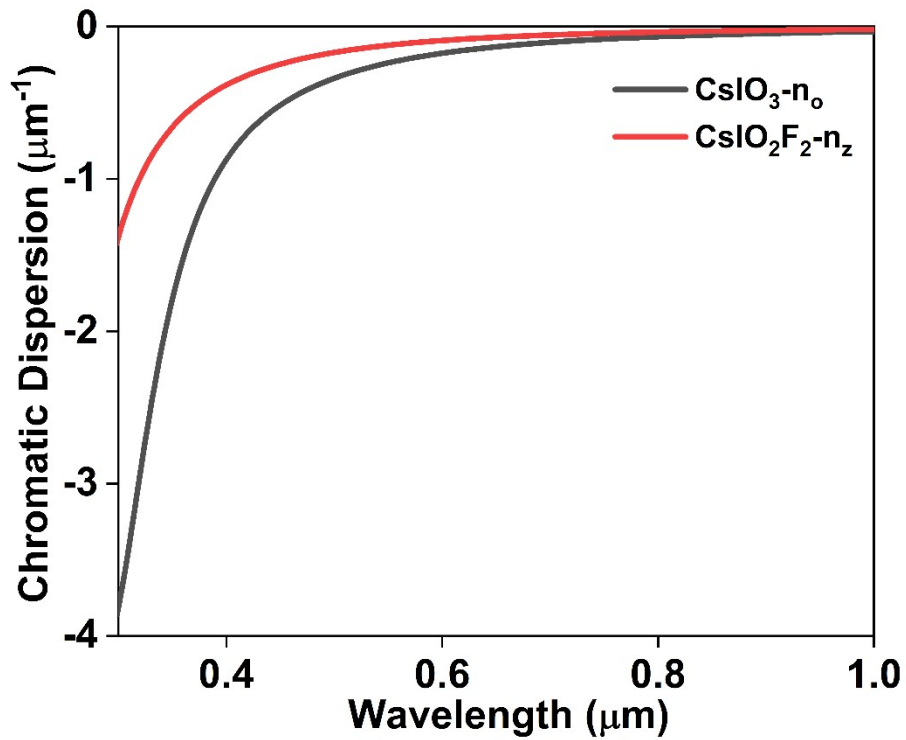


Figure S8. The Chromatic dispersion of  $\text{CsIO}_3$  and  $\text{CsIO}_2\text{F}_2$ .

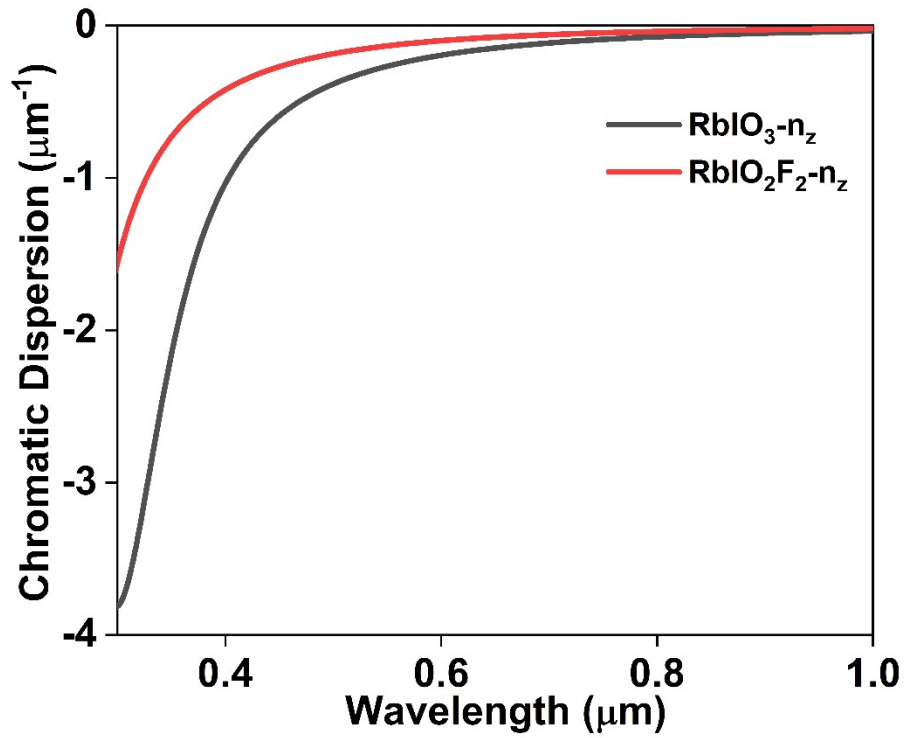


Figure S9. The Chromatic dispersion of  $\text{RbIO}_3$  and  $\text{RbIO}_2\text{F}_2$ .

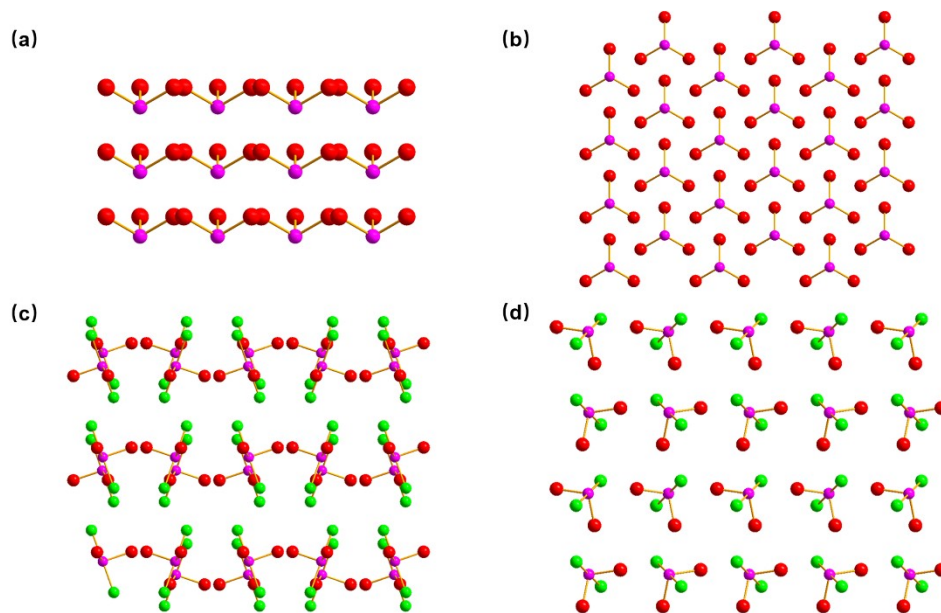


Figure S10. (a)  $\text{KIO}_3$  refractive index direction (210) structural alignment. (b) Structural alignment of  $\text{KIO}_3$  in the direction of refractive index (001). (c)  $\text{KIO}_2\text{F}_2$  refractive index direction (001) structural arrangement. (d) Structural alignment of  $\text{KIO}_2\text{F}_2$  in the direction of refractive index (010). O (Red) , I (Pink) ,F (Bright Green).

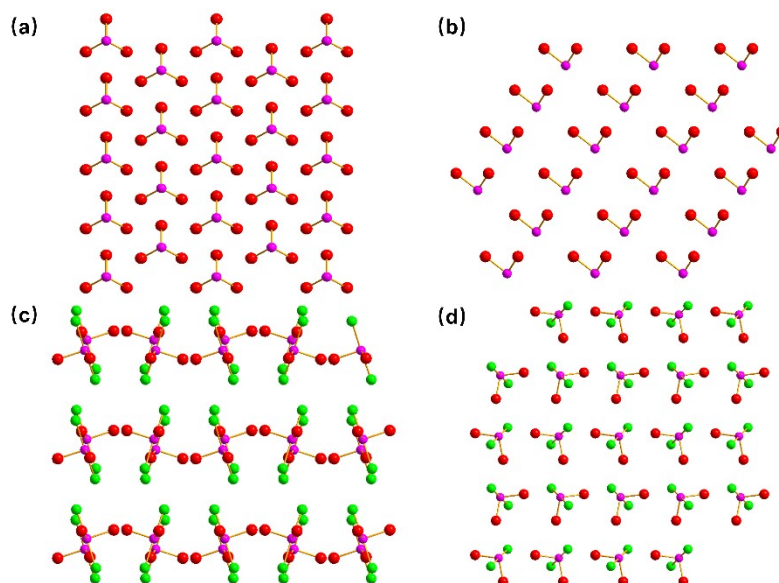


Figure S11. (a)  $\text{RbIO}_3$  refractive index direction (001) structural alignment. (b) Structural alignment of  $\text{RbIO}_3$  in the direction of refractive index (010). (c)  $\text{RbIO}_2\text{F}_2$  refractive index direction (001) structural arrangement. (d) Structural alignment of  $\text{RbIO}_2\text{F}_2$  in the direction of refractive index (010). O (Red), I (Pink), F (Bright Green).

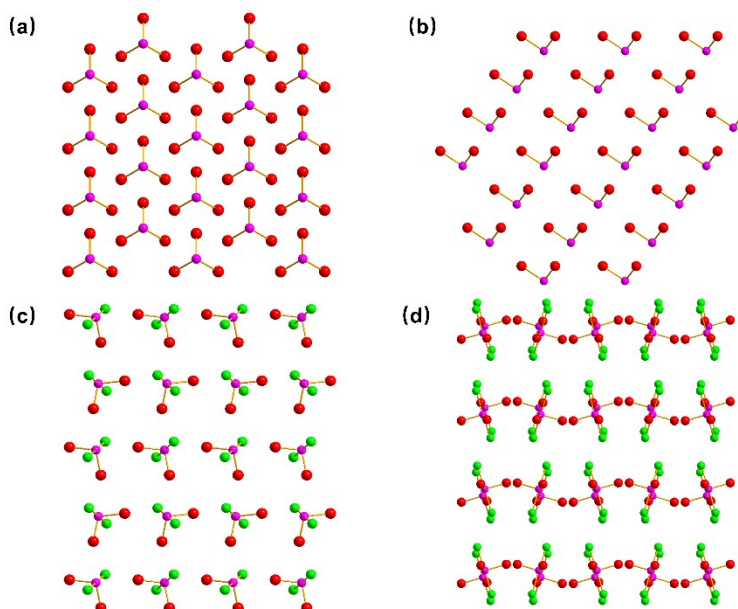


Figure S11. (a)  $\text{CsIO}_3$  refractive index direction (001) structural alignment. (b) Structural alignment of  $\text{CsIO}_3$  in the direction of refractive index (010). (c)  $\text{CsIO}_2\text{F}_2$  refractive index direction (010) structural arrangement. (d) Structural alignment of  $\text{CsIO}_2\text{F}_2$  in the direction of refractive index (001). O (Red), I (Pink), F (Bright Green).



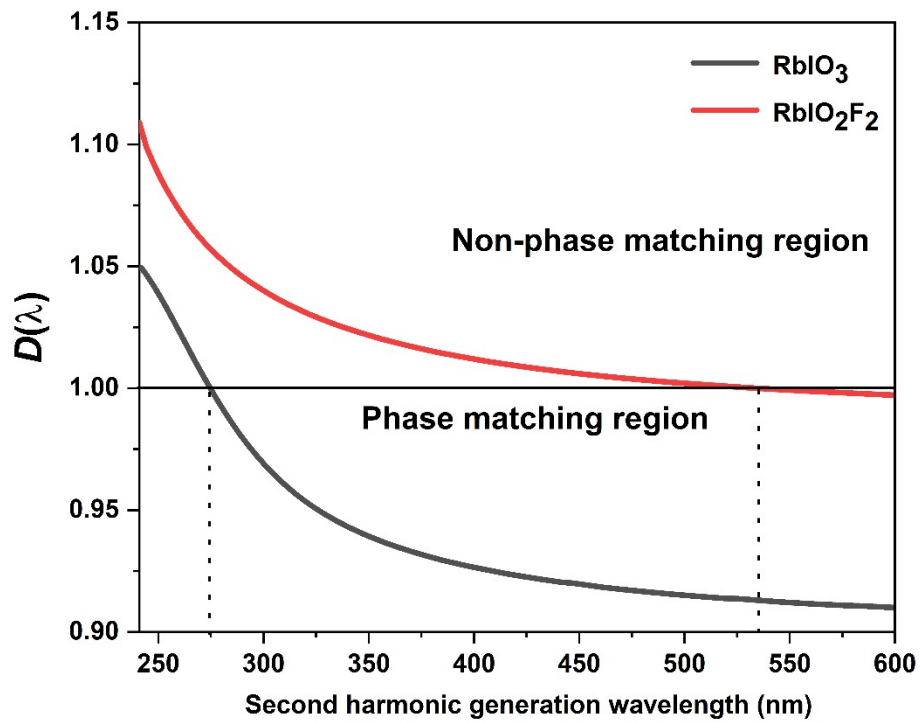


Figure S12. Refractive index dispersion of different NLO iodates, from  $\text{RbIO}_3$  and  $\text{RbIO}_2\text{F}_2$ .

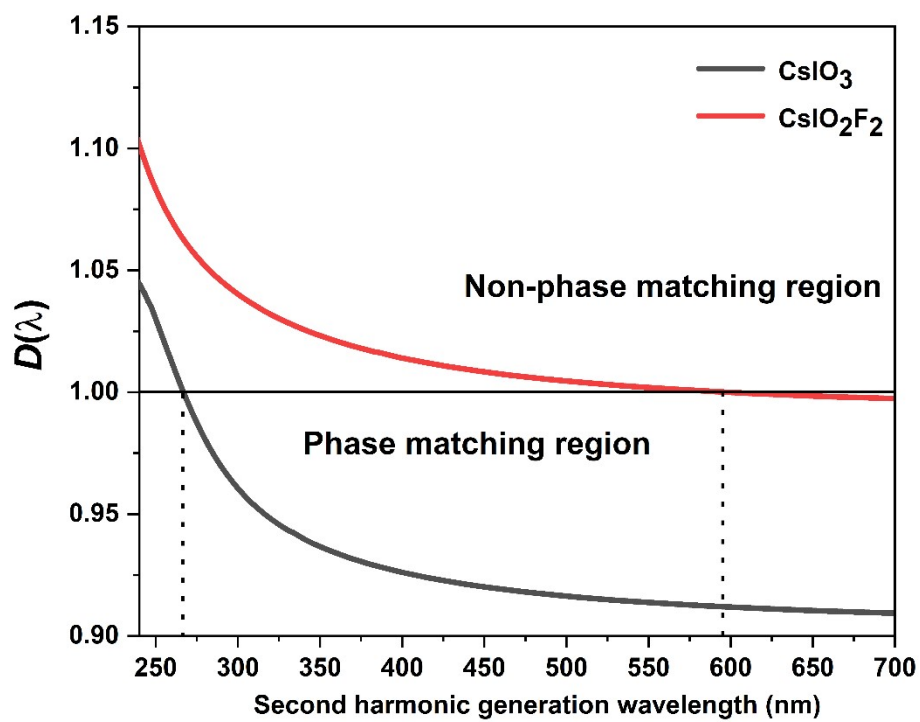




Figure S13. Refractive index dispersion of different NLO iodates, from CsIO<sub>3</sub> and CsIO<sub>2</sub>F<sub>2</sub>.

## References

1. C. Svensson and K. Ståhl, The crystal structure of NaIO<sub>3</sub> at 293 K, *J. Solid. State. Chem.*, 1988, **77**, 112-116.
2. J.-P. Laval and N. Jennene Boukharrata, Sodium iodine (V) oxyfluoride, NaIO<sub>2</sub>F<sub>2</sub>, *Acta Crystallogr. C.*, 2008, **64**, 147-149.
3. E. L. Belokoneva, S. Y. Stefanovich and O. V. Dimitrova, New nonlinear optical potassium iodate K[IO<sub>3</sub>] and borates K<sub>3</sub>[B<sub>6</sub>O<sub>10</sub>]Br, KTa[B<sub>4</sub>O<sub>6</sub>(OH)<sub>4</sub>](OH)<sub>2</sub>· 1.33 H<sub>2</sub>O—Synthesis, structures and relation to the properties, *J. Solid. State. Chem.*, 2012, **195**, 79-85.
4. S. Abrahams and J. Bernstein, Ferroelastic KIO<sub>2</sub>F<sub>2</sub>: Crystal structure and ferroelastic transformation, *J Chem. Phys.*, 1976, **64**, 3254-3260.
5. Q. Wu, H. Liu, F. Jiang, L. Kang, L. Yang, Z. Lin, Z. Hu, X. Chen, X. Meng and J. Qin, RbIO<sub>3</sub> and RbIO<sub>2</sub>F<sub>2</sub>: Two promising nonlinear optical materials in mid-IR region and influence of partially replacing oxygen with fluorine for improving laser damage threshold, *Chem. Mater.*, 2016, **28**, 1413-1418.
6. M. Zhang, C. Hu, T. Abudouwufu, Z. Yang and S. Pan, Functional materials design via structural regulation originated from ions introduction: A study case in cesium iodate system, *Chem. Mater.*, 2018, **30**, 1136-1145.